

Detection of Free Monomeric Silver(I) and Gold(I) Cyanides, AgCN and AuCN: Microwave Spectra and Molecular Structure

Toshiaki Okabayashi,^{*,†} Emi Y. Okabayashi,[‡] Fumi Koto,[‡] Toshimasa Ishida,[§] and Mitsutoshi Tanimoto^{||}

Graduate School of Science and Technology, Shizuoka University, 836 Oya, Suruga-ku, Shizuoka 422-8529, Japan, Department of Chemistry, Faculty of Science, Shizuoka University, 836 Oya, Suruga-ku, Shizuoka 422-8529, Japan, Fukui Institute for Fundamental Chemistry, Kyoto University, 34-4 Takano-Nishihiraki-cho, Sakyou-ku, Kyoto 606-8103, Japan, and Department of Chemistry, Faculty of Science, Kanagawa University, 2946 Tsuchiya, Hiratsuka 259-1293, Japan

Received October 20, 2008; E-mail: sctokab@ipc.shizuoka.ac.jp

Abstract: The chemistry of the group 11 metal cyanide system has been of considerable interest because of the commercial importance of some of the complexes formed in this system. These metal cyanides contain one-dimensional linear $-M-CN-M-CN-M-$ chains in the solid state; however, they have not been observed as free monomeric species. This Article reports the first detection of monomeric AgCN and AuCN in the gas phase by using rotational spectroscopy. The sputtering reaction of silver and/or gold sheets placed on a stainless steel cathode with CH_3CN diluted in Ar resulted in the production of AgCN and AuCN spectra. Spectroscopic observation of the parent and several rare isotopic species allowed the determination of r_0 , r_s , r_{le} , $r_m^{(1)}$, and $r_m^{(2)}$ structures in the case of AgCN and r_0 and r_s structures in the case of AuCN. All data indicate that these two species have a linear MCN geometry with a low-energy bending vibration.

Introduction

The chemistry of the group 11 metal cyanide system has been of considerable interest because of the commercial importance of the complexes formed in this system. For example, anionic silver and gold cyanides, $[Ag(CN)_2]^-$ and $[Au(CN)_2]^-$, are among the very few soluble compounds of these metals, and cyanides are thus used in mining as well as in electroplating and photography. In the so-called cyanide process, an ore is mixed with a cyanide, and the noble-metal cations are complexed by the cyanide anions to form soluble derivatives. Studies on the mechanism of these processes have suggested MCN as a probable intermediate.¹

The study of AuCN is of considerable interest because the pronounced local maximum of the relativistic effect and the contraction of the 6s shell make gold a unique element.² To understand its unique chemical properties attributed to relativity, many theoretical studies have been carried out on simple singlet gold compounds. In particular, recent developments in computer technology have enabled a large-scale relativistic quantum-chemical calculation for such species. However, it is still difficult to carry out the rigorous calculations required to predict precise parameters in Au compounds. Hence, high-resolution spectroscopic studies on such species are highly desired for the further development of the relativistic quantum-chemical calculation.

Although the structures of monomeric AgCN and AuCN are not well understood, several experimental studies have been carried out on the solid-state structures of these compounds using X-ray³ and neutron diffraction,^{4–6} and infrared⁴ and NMR spectroscopy.⁷ These works have revealed that both solid AgCN and solid AuCN exist as infinite linear chains of alternating metal and cyanide moieties, $-M-CN-M-CN-M-$. For solid AgCN, ¹³C MAS NMR study also revealed that approximately 30% of the silver sites are disordered ($-CN-Ag-NC-$ or $-NC-Ag-CN-$) and that the remaining 70% of sites are ordered ($-CN-Ag-CN-$).⁷ Another group 11 monocyanoide, CuCN, has also been studied by X-ray^{8–10} and neutron diffraction,^{4,11} and infrared,⁴ NMR/NQR,¹² and EXAFS spectroscopy.¹³ These studies suggested that one polymorph of CuCN, α -CuCN, adopts the same linear chain structure as

- (3) Zhdanov, G. S.; Shugam, E. A. *Zh. Fiz. Khim.* **1945**, *19*, 519.
- (4) Bowmaker, G. A.; Kennedy, B. J.; Reid, J. C. *Inorg. Chem.* **1998**, *37*, 3968.
- (5) Hibble, S. J.; Cheyne, S. M.; Hannon, A. C.; Eversfield, S. G. *Inorg. Chem.* **2002**, *41*, 1042.
- (6) Hibble, S. J.; Hannon, A. C.; Cheyne, S. M. *Inorg. Chem.* **2003**, *42*, 4724.
- (7) Bryce, D. L.; Wasylishen, R. E. *Inorg. Chem.* **2002**, *41*, 4131.
- (8) Norberg, B.; Jacobson, B. *Acta Chem. Scand.* **1949**, *3*, 174.
- (9) Cromer, D. T.; Douglass, R. M.; Staritzky, E. *Anal. Chem.* **1957**, *29*, 316.
- (10) Wang, J.; Collins, M. F.; Johari, G. P. *Phys. Rev. B* **2002**, *65*, 180103.
- (11) Hibble, S. J.; Cheyne, S. M.; Hannon, A. C.; Eversfield, S. G. *Inorg. Chem.* **2002**, *41*, 4990.
- (12) Kroeker, S.; Wasylishen, R. E.; Hanna, J. V. *J. Am. Chem. Soc.* **1999**, *121*, 1582.
- (13) Stemmler, T. L.; Barnhart, T. M.; Penner-Hahn, J. E.; Tucker, C. E.; Knochel, P.; Böhme, M.; Frenking, G. *J. Am. Chem. Soc.* **1995**, *117*, 12489.

[†] Graduate School of Science and Technology, Shizuoka University.

[‡] Faculty of Science, Shizuoka University.

[§] Kyoto University.

^{||} Kanagawa University.

(1) Puddephatt, R. J. In *Comprehensive Coordination Chemistry*; Wilkinson, G., Ed.; Pergamon: Oxford, UK, 1987; Vol. 5, p 861.
 (2) Pykkö, P. *Angew. Chem., Int. Ed.* **2004**, *43*, 4412.

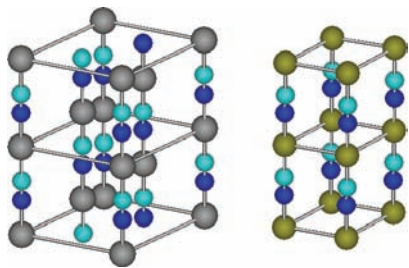


Figure 1. Crystal structures of AgCN (left) and AuCN (right) determined by neutron diffraction.^{5,6}

AgCN, albeit in an even more highly disordered form.¹¹ However, the structures of α -CuCN/AgCN and AuCN differ in the way the chains are packed together (Figure 1). In AuCN, gold atoms are arranged in layers, whereas in α -CuCN/AgCN, copper/silver atoms in neighboring chains are displaced along the chain axis by one-third of the chain repeat distance. It is thought that AuCN adopts this chain arrangement to minimize the Au–Au distance and to enhance an aurophilic interaction.⁴ This interaction is thought to result from electron correlation of the closed-shell component, somewhat similarly to van der Waals interactions, but it is unusually strong as a result of relativistic effects.^{14,15} Recently, Pyykkö and co-workers have theoretically predicted that CuCN, AgCN, and AuCN may have an alternative sheet structure with energy comparable to that of the chain structure.^{16,17}

In contrast, there have been very few studies on monomeric silver and gold monocyanoes, AgCN and AuCN. Monomeric copper monocyanoide, CuCN, has been experimentally detected by microwave spectroscopy.¹⁸ Five theoretical studies have so far been reported on AgCN and AuCN. In 1993, Veldkamp and Frenking¹⁹ predicted that the ground electronic states of AgCN and AuCN were the closed-shell $^1\Sigma^+$ states. In 1999, Seminario et al.²⁰ carried out density-functional-theory (DFT) calculations on several gold-bearing species including AuCN. Later, Dietz et al.²¹ concluded that the cyanide forms, MCN, of the group 11 metals (Cu, Ag, and Au) were several thousand cm^{-1} more stable than the isocyanide forms, MNC, of these metals. Lee et al.²² extensively studied the group 1 (Li, Na, K, Rb, Cs, and Fr) and group 11 (Cu, Ag, and Au) monocyanoes and discussed the stability of their linear-MCN, linear-MNC, and triangular isomers. Recently, Zaleski-Ejgierd et al.²³ carried out high-precision calculations on MCN ($M = \text{Cu, Ag, Au, and Rg}$) at the CCSD(T) level with the latest pseudopotentials and basis sets up to cc-pVQZ. However, experimental evidence for monomeric AgCN and AuCN is considerably scarce. The photoelectron spectroscopy of AgCN (and also CuCN)²⁴ is the sole experimental study on the subject.

(14) Schmidbaur, H. *Chem. Soc. Rev.* **1995**, *24*, 391.

(15) Schmidbaur, H. *Gold Bull.* **2000**, *33*, 3.

(16) Hakala, M. O.; Pyykkö, P. *Chem. Commun.* **2006**, 2890.

(17) Zaleski-Ejgierd, P.; Hakala, M.; Pyykkö, P. *Phys. Rev. B* **2007**, *76*, 094104.

(18) Grotjahn, D. B.; Brewster, M. A.; Ziurys, L. M. *J. Am. Chem. Soc.* **2002**, *124*, 5895.

(19) Veldkamp, A.; Frenking, G. *Organometallics* **1993**, *12*, 4613.

(20) Seminario, J. M.; Zacarias, A. G.; Tour, J. M. *J. Am. Chem. Soc.* **1999**, *121*, 411.

(21) Dietz, O.; Rayón, V. M.; Frenking, G. *Inorg. Chem.* **2003**, *42*, 4977.

(22) Lee, D.; Lim, I. S.; Lee, Y. S.; Hagebaum-Reignier, D.; Jeung, G.-H. *J. Chem. Phys.* **2007**, *126*, 244313.

(23) Zaleski-Ejgierd, P.; Patzschke, M.; Pyykkö, P. *J. Chem. Phys.* **2008**, *128*, 224303.

(24) Boldyrev, A. I.; Li, X.; Wang, L.-S. *J. Chem. Phys.* **2000**, *112*, 3627.

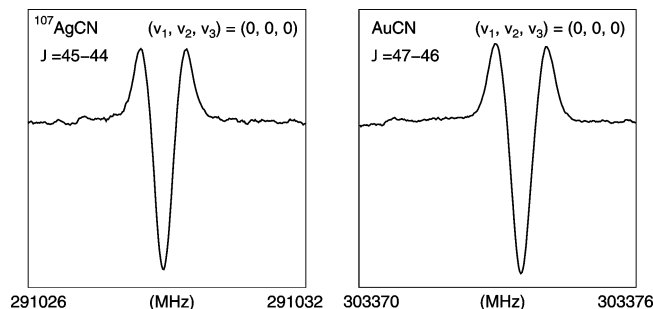


Figure 2. A typical spectral line of $^{107}\text{AgCN}$ and AuCN in the ground vibrational states generated by a sputtering reaction of a silver and gold sheet, respectively. The integration time is approximately 10 s for each spectrum.

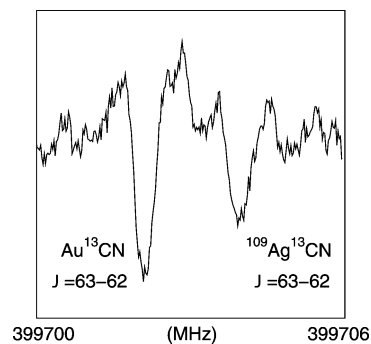


Figure 3. Spectral lines of Au^{13}CN and $^{109}\text{Ag}^{13}\text{CN}$ near 399.7 GHz, $J = 63-62$, generated by a sputtering reaction of gold and silver sheets with $\text{CH}_3^{13}\text{CN}$. The integration time is approximately 10 s. Experimental conditions were not optimized to save the ^{13}C -enriched precursor.

This Article reports on the first preparation of free silver and gold monocyanoes, AgCN/AuCN, and the observation of their rotational spectra. The AgCN/AuCN molecules have been generated by the sputtering reaction of Ag/Au sheets placed on a stainless steel cathode in the presence of acetonitrile (CH_3CN) vapor. Accurate bond lengths in both species have been determined from the isotopic data. Reliability of various theoretical calculations has been assessed for the first time through a comparison between experimental and theoretical results.

Experimental Details and Data Analysis

The present experiments were carried out using a source-modulation microwave spectrometer with a free space discharge cell.²⁵ A multiplier following an OKI klystron was employed as the microwave source. The radiation transmitted through the cell was detected by an InSb detector cooled by liquid He. The accuracy of observed transition frequencies was better than 30 kHz.

The AgCN and AuCN species were generated in the free space cell by a sputtering reaction. Vapor of CH_3CN entrained in argon gas was continuously introduced into the cell. Silver and/or gold sheets lining the inner surface of the stainless steel cathode were sputtered by a dc glow discharge with a current of 300 mA in the presence of 1 mTorr of CH_3CN vapor and 4 mTorr of Ar gas. For observing the ^{13}C or ^{15}N isotopic species, we used, instead of normal $\text{CH}_3^{12}\text{C}^{14}\text{N}$ species, $\text{CH}_3^{13}\text{CN}$ or CH_3^{15}N as the precursor. The cell was cooled to approximately 150 K by circulating liquid nitrogen. Under these conditions, the AgCN and AuCN lines were strong enough to be observed without data accumulation. The typical spectra obtained are shown in Figures 2 and 3. The AgCN and AuCN lines showed diamagnetic properties, and they rapidly disappeared when the discharge current was turned off. This behavior indicated that the carriers were singlet transient species. Weaker transitions were also observed in the ν_2 (bend) vibrational

Table 1. Molecular Constants of AgCN and AuCN^a

species	state	B_v (MHz)	D_v (kHz)	H_v (mHz)	q_2 (MHz)	q_{vJ} (kHz)
¹⁰⁷ Ag ¹² C ¹⁴ N	ground	3237.56180(23)	0.96389(11)	−0.077(14)		
	$\nu_2 = 1$	3255.21556(10)	1.012551(29)	−0.077 ^b	3.77943(20)	−0.012342(57)
	$\nu_3 = 1$	3223.27592(19)	0.957235(50)	−0.077 ^b		
¹⁰⁹ Ag ¹² C ¹⁴ N	ground	3226.58872(27)	0.95758(12)	−0.082(17)		
	$\nu_2 = 1$	3244.17954(15)	1.005964(44)	−0.082 ^b	3.75465(31)	−0.012239(87)
	$\nu_3 = 1$	3212.35454(14)	0.951011(37)	−0.082 ^b		
¹⁰⁷ Ag ¹³ C ¹⁴ N	ground	3190.83488(15)	0.944814(72)	−0.0931(96)		
¹⁰⁹ Ag ¹³ C ¹⁴ N	ground	3179.70596(20)	0.938679(98)	−0.070(13)		
¹⁰⁷ Ag ¹² C ¹⁵ N	ground	3097.58711(16)	0.873505(71)	−0.0525(89)		
¹⁰⁹ Ag ¹² C ¹⁵ N	ground	3086.758391(64)	0.867485(29)	−0.0780(36)		
¹⁹⁷ Au ¹² C ¹⁴ N	ground	3230.21115(18)	0.640370(83)	−0.093(12)		
	$\nu_2 = 1$	3242.18930(11)	0.660642(32)	−0.093 ^b	2.86427(22)	−0.004587(65)
¹⁹⁷ Au ¹³ C ¹⁴ N	ground	3177.20793(13)	0.625790(62)	−0.0699(82)		
¹⁹⁷ Au ¹² C ¹⁵ N	ground	3079.73540(12)	0.576615(55)	−0.0642(69)		

^a Values in parentheses indicate one standard deviation. ^b Fixed to the ground-state values in the analysis.

state of both AgCN and AuCN and in the ν_3 (Ag–C str.) vibrational state of AgCN. Much weaker transitions in more highly excited vibrational states were not detected due to poor signal-to-noise ratio. In total, 196 lines of six AgCN isotopomers and 101 lines of three AuCN isotopomers were observed in the frequency range between 77 and 402 GHz.

The observed spectra showed a typical pattern of a linear molecule in the $^1\Sigma$ state. Transition frequencies were analyzed using the standard rotational energy formula for a linear molecule:

$$E_{vJ} = B_v[J(J+1) - l^2] - D_v[J(J+1) - l^2]^2 + H_v[J(J+1) - l^2]^3 \pm \frac{1}{2}[q_v + q_{vJ}J(J+1)]J(J+1) \quad (1)$$

where v and l are the quantum numbers of the bending vibration. The value of l was set to zero in the ground and ν_3 states and one in the ν_2 state. The last term in eq 1, which should be neglected for the ground and ν_3 states, accounts for the l -type doubling in the ν_2 state. The q_v value of a linear triatomic molecule usually has a positive value, and the + and − signs in eq 1 correspond to the f and e levels, respectively. An analysis of the rotational transitions led to the molecular constants listed in Table 1. The observed rotational transition frequencies and the residuals of the fit are summarized in Tables S1 and S2. The standard deviations of the fits, 10–20 kHz for the ground and vibrationally excited states of each isotopomer, are reasonable in view of the expected measurement error. The variations in the rotational constants due to isotopic substitutions indicate that the carriers of the microwave spectra are monocyanides (AgCN and AuCN), and not monoisocyanides (AgNC and AuNC).

Computational Details

Geometry optimizations and vibrational calculations were carried out using a Gaussian 03 program package.²⁶ The DFT calculations at B3PW91 level of theory (the Becke-style three-parameter Density Functional Theory with Perdew–Wang's 91 expression²⁷) were performed on CuCN, AgCN, and AuCN molecules in their ground electronic states, $X^1\Sigma^+$. The 6-311++G(3df) basis set was used for C and N, while LanL2DZ basis set (Los Alamos effective core potential²⁸ plus DZ) was used for the metal atoms.

Results and Discussion

Vibrational Frequency. The present measurement has led to the first determination of the molecular constants of AgCN

in the ground, ν_2 , and ν_3 vibrational states and those of AuCN in the ground and ν_2 vibrational states. The harmonic vibrational frequencies of the lower stretching vibration ν_3 (Ag–C str./Au–C str.) are estimated as

$$\omega_3 \approx \left(\frac{4B_c^3}{D_e} \right)^{1/2} \quad (2)$$

in a diatomic approximation.²⁹ When the rotational and centrifugal distortion constants in the equilibrium state were approximated by those in the ground state, the vibrational frequencies were calculated to be $\omega_3 \approx 400 \text{ cm}^{-1}$ in AgCN and 480 cm^{-1} in AuCN. The corresponding value of CuCN was reported to be 478 cm^{-1} through microwave spectroscopy.¹⁸

The harmonic vibrational frequency of the bending vibration ν_2 is estimated from the l -type doubling constant q_2 by using the following equation:²⁹

$$\omega_2 \approx \frac{2.6B_c^2}{q_2} \quad (3)$$

The molecular constants given in Table 1 yielded the vibrational frequencies to be $\omega_2 \approx 240 \text{ cm}^{-1}$ for AgCN and 320 cm^{-1} for AuCN, whereas $\omega_2 \approx 270 \text{ cm}^{-1}$ was reported for CuCN.¹⁸ These ω_2 and ω_3 frequencies are compared to the previous experimental and theoretical results in Table 2. The ω_3 energies of both CuCN and AgCN determined by photoelectron spectroscopy²⁴ were, despite a large experimental error, in agreement with the microwave estimation.

The bending vibrational energies in the solid state have two values, higher $\delta(\text{MCN})$ and lower $\delta(\text{CNM})$,⁴ whereas the monomer has a single $\angle\text{MCN}$ bending vibration energy, ω_2 . The present ω_2 values fall between the $\delta(\text{MCN})$ and $\delta(\text{CNM})$ values in the solid state.⁴ In the solid state, the $\angle\text{MCN}$ and $\angle\text{CNM}$ bending modes of the linear chain (–M–CN–M–CN–M–) probably have similar vibrational energies and thus are strongly coupled. As a result of the vibrational coupling, the $\angle\text{MCN}$ energy is increased and the $\angle\text{CNM}$ energy decreased. This vibrational coupling likely causes a difference between the bending vibrational energies in the solid and gaseous phases.

Similar coupling also explains the large differences in the M–C vibration between the solid and gaseous phases. The M–C stretching vibrational energies in the solid state⁴ were

(25) Okabayashi, T.; Tanimoto, M. *J. Chem. Phys.* **1993**, *99*, 3268.

(26) Frisch, M. J. *Gaussian 03*, revision B.05; Gaussian, Inc.: Pittsburgh, PA, 2003.

(27) Perdew, J. P.; Wang, Y. *Phys. Rev. B* **1992**, *45*, 13244.

(28) Hay, P. J.; Wadt, W. R. *J. Chem. Phys.* **1985**, *82*, 299.

(29) Townes, C. H.; Schawlow, A. L. *Microwave Spectroscopy*; McGraw-Hill: New York, 1955.

Table 2. Vibrational Frequencies of CuCN, AgCN, and AuCN (cm^{-1})

molecule	$\nu_1(\text{C-N str.})$	$\nu_2(\text{bend})$	$\nu_3(\text{M-C str.})$	methods	ref	
CuCN		270	478	MW	18	
			480(30)	PE	24	
	2263	271	460	B3PW91/6-311++G(3df)/LanL2DZ	this work	
	2204	255	483	CCSD(T)/cc-pVQZ	23	
	2190	336	519	CCSD(T)	22	
	2177	255	512	BP86/TZP	21	
	2249	251	465	B3LYP/6-311+G*	24	
	2079	245	479	MP2/6-311+G*	24	
	2159	225	453	CCSD(T)/6-311+G*	24	
	CuCN(solid)	2170	168/326	IR	4	
AgCN		240	400	MW	this work	
			390(30)	PE	24	
	2264	236	382	B3PW91/6-311++G(3df)/LanL2DZ	this work	
	2203	221	402	CCSD(T)/cc-pVQZ	23	
	2168	186	395	CCSD(T)	22	
	2171	224	397	BP86/TZP	21	
	2094	182	364	MP2/DZP	19	
	AgCN(solid)	2164	112/272	IR	4	
	AuCN		320	480	MW	this work
				476	B3PW91/6-311++G(3df)/LanL2DZ	this work
2276		313	476	B3PW91/6-311++G(3df)/LanL2DZ	this work	
2215		289	482	CCSD(T)/cc-pVQZ	23	
2127		309	520	MP2/cc-pVQZ	23	
2179		259	478	CCSD(T)	22	
2176		292	475	BP86/TZP	21	
2105		279	464	MP2/DZP	19	
AuCN(solid)		2236	224/358	IR	4	

clearly larger than the corresponding ω_3 values in the gas phase by $80\text{--}120\text{ cm}^{-1}$. As in the bending vibrations, the higher M–C stretching frequency is increased and the lower N–M frequency decreased. Because the motion of the M–C stretching is probably similar to that of the N–M stretching, the coupled vibrational mode with the higher energy is consequently nearly antisymmetric (infrared active), and that with lower energy is symmetric (infrared inactive). Thus, only the M–C stretching mode of the higher energy was observed in the solid state.

The present DFT calculation using the B3PW91 method with the modest 6-311++G(3df) and LanL2DZ basis sets accurately reproduced the experimental frequencies of MCN. Recent accurate CCSD(T) calculations by Zaleski-Ejgierd et al.²³ provided ω_3 values close to the experimental ones for CuCN, AgCN, and AuCN. They also gave good ω_2 estimates for CuCN and AgCN, but slightly smaller ω_2 for AuCN. In contrast, their MP2 calculation²³ provided ω_2 values comparable to the present ones, but slightly larger ω_3 energies. As shown in Table 2, most of the earlier calculations^{21,22,24} yielded accurate estimates for ω_3 and rather poor values for ω_2 . An observation of the infrared spectrum of the monomeric MCN, which would provide precise vibrational energies, is highly desired.

It is beneficial to compare the molecular properties, like vibrational frequencies, potential functions, and bond lengths, with those of the isoelectronic molecules. Such molecules have the same number of valence electrons in similar molecular orbitals of different shapes. One of the best-known cases is hydrogen cyanide, HCN, and its isoelectronic species, HBF⁺, HBO, HCO⁺, HNN⁺, HNC, and HOC⁺.^{30,31} The group 10 monocarbonyls M'CO (M' = Ni, Pd, and Pt) are isoelectronic with the group 11 metal cyanides MCN (M = Cu, Ag, and Au). The vibrational frequencies of metal cyanides MCN are compared here to those of their isoelectronic monocarbonyls M'CO. Figure 4 shows the changes in the ω_2 (bend) and ω_3 (M–C str.) values of the two groups of species. For both ω_2 and ω_3 , the group 10 monocarbonyls have larger vibrational frequencies than do the group 11 monocyanides. In the group 10 monocarbonyls, chemical bonding between the metal and

carbon atoms is enhanced due to the M $d\pi \rightarrow$ CO $p\pi^*$ back-donation. Because this back-donation is strongly affected by the nature of the metal, the vibrational frequencies are scattered in the group 10 monocarbonyls. In contrast, those of the group 11 monocyanides do not largely change, because the chemical bond between a group 11 metal and a cyano group is mainly constructed by a σ bond that is not drastically affected by the nature of the metal atom.

Molecular Structure. Table 3 lists the bond lengths of AgCN and AuCN as well as those of CuCN,¹⁸ obtained by several methods,^{32–34} r_0 , r_s , r_{Te} , $r_{\text{m}}^{(1)}$, and $r_{\text{m}}^{(2)}$, along with several recent theoretical predictions. The uncertainties given for the AgCN and AuCN structures are estimated from those of the fundamental constants and the observed rotational constants listed in Table 1. The experimental equilibrium bond length, r_e , has not been obtained from the present rotational constants because of the lack of vibrationally excited data. Because the $r_{\text{m}}^{(2)}$ method often provides a good estimate of the equilibrium structure,³⁴ the $r_{\text{m}}^{(2)}$ values for CuCN and AgCN are used for qualitative

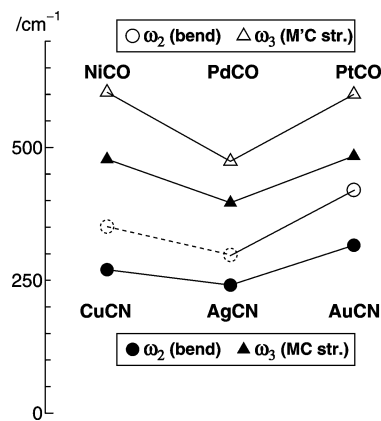


Figure 4. Comparison of the vibrational frequencies in the group 10 monocarbonyls M'CO (M' = Ni,³⁵ Pd,³⁶ and Pt^{37,38}) and the isoelectronic group 11 metal cyanides MCN (M = Cu,¹⁸ Ag, and Au) and the isoelectronic group 10 monocarbonyls M'CO (M' = Ni,³⁵ Pd,³⁶ and Pt^{37,38}). The ω_2 values for NiCO and PdCO refer to theoretical calculations.^{39,40}

Table 3. Molecular Structures of CuCN, AgCN, and AuCN (pm)

molecule		$r(\text{M}-\text{C})$	$r(\text{C}\equiv\text{N})$	methods	ref	
CuCN	r_0	183.231(7)	115.76(1)	MW	18	
	r_s	183.284(4)	115.669(3)	MW	18	
	$r_m^{(2)}$	182.962(4)	116.213(3)	MW	18	
	r_e	183.84	115.73	B3PW91/6-311++G(3df)/LanL2DZ	this work	
	r_e	181.85	116.39	CCSD(T)/cc-pVQZ	23	
	r_e	182.36	116.40	CCSD(T)/cc-pVQZ with SO/BSSE	23	
	r_e	184.0	117.0	CCSD(T)	22	
	r_e	177.8	116.8	BP86/TZP	21	
	r_e	185.3	116.1	B3LYP/6-311+G*	24	
	r_e	182.6	118.2	MP2/6-311+G*	24	
	r_e	186.3	117.7	CCSD(T)/6-311+G*	24	
	r	184.6	117.0	ND	11	
	α -CuCN(solid)					
AgCN	r_0	203.324(45)	115.527(67)	MW ^a	this work	
	r_s	203.4182(27)	115.4733(20)	MW ^a	this work	
	r_{I_e}	203.476(36)	115.477(28)	MW ^a	this work	
	$r_m^{(1)}$	203.562(53)	115.525(26)	MW ^a	this work	
	$r_m^{(2)}$	203.1197(23)	116.0260(26)	MW ^a	this work	
	r_e	203.73	115.65	B3PW91/6-311++G(3df)/LanL2DZ	this work	
	r_e	202.04	116.33	CCSD(T)/cc-pVQZ	23	
	r_e	202.42	116.40	CCSD(T)/cc-pVQZ with SO/BSSE	23	
	r_e	203.0	117.0	CCSD(T)	22	
	r_e	201.4	116.7	BP86/TZP	21	
	r_e	208.7	118.8	MP2/DZP	19	
	r	206	116	ND	5	
	AgCN(solid)					
AuCN	r_0	191.251(16)	115.856(24)	MW ^a	this work	
	r_s	191.22519(84)	115.86545(97)	MW ^a	this work	
	r_e	191.51	115.56	B3PW91/6-311++G(3df)/LanL2DZ	this work	
	r_e	191.12	116.23	CCSD(T)/cc-pVQZ	23	
	r_e	191.05	116.23	CCSD(T)/cc-pVQZ with SO/BSSE	23	
	r_e	186.51	116.92	MP2/cc-pVQZ	23	
	r_e	192.0	117.0	CCSD(T)	22	
	r_e	192.0	116.8	BP86/TZP	21	
	r_e	192.2	115.9	B3PW91/LanL-E	20	
	r_e	192.9	118.7	MP2/DZP	19	
	r	197.17(5)	115.47(4)	ND	6	
	AuCN(solid)					

^a The uncertainties given for the AgCN and AuCN results are estimated from those of the fundamental constants and the observed rotational constants listed in Table 1.

discussions. However, because there are no stable gold isotopes besides ¹⁹⁷Au, only the r_0 and r_s structures are experimentally available for AuCN. Hence, the r_s values are used for qualitative discussions. The present r_s values appear reasonable because $r_s(\text{C}\equiv\text{N})$ of AuCN is close to $r_m^{(2)}(\text{C}\equiv\text{N})$ of CuCN and AgCN.

The $\text{C}\equiv\text{N}$ lengths in the solid state^{5,6,11} are close to the corresponding values in the gas phase, which means that the cyano group exists as an almost pure CN^- ion in both phases. On the other hand, the $\text{M}-\text{C}$ lengths clearly differ. While the $\text{Cu}-\text{C}$ length in the solid state is close to that in the gas phase, the $\text{Ag}-\text{C}$ length is about 3 pm longer in the solid state. For AuCN, the corresponding difference is as large as 6 pm. For solid structure determination,^{5,6,11} it was assumed that the $\text{M}-\text{C}$ length had the same value as the $\text{N}-\text{M}$ length; that is, their

values are thus averaged values of somewhat shorter $\text{M}-\text{C}$ and longer $\text{N}-\text{M}$ lengths. This is probably a major reason why the solid-state values are longer than the gaseous ones.

It is also possible that the aurophilic interaction^{14,15} explains the rather large difference of $\text{M}-\text{C}$ seen in AuCN. In solid AuCN, it is thought that a gold atom is weakly bonded to six nearby gold atoms. Typical aurophilic interaction energy is thought to be 29–46 kJ/mol and is comparable with a good hydrogen bond.² Thus, it is estimated that the $\text{M}-\text{C}$ and $\text{N}-\text{M}$ lengths are lengthened in the solid state to reduce the $\text{Au}-\text{Au}$ distance between the $-\text{Au}-\text{CN}-\text{Au}-\text{CN}-\text{Au}-$ chains.

The present DFT calculation using the B3PW91 method well reproduced the experimental internuclear distances of MCN. Recent accurate CCSD(T) calculations with the large cc-pVQZ basis set by Zaleski-Ejgierd et al.²³ also provided consistent values. Most of the other $\text{M}-\text{C}$ distances calculated using a fairly large basis set^{19–22,24} were also close to the experimental lengths. Early MP2/I work,¹⁹ where the basis set I was essentially the DZP basis set with relativistic effective core potential, supplied poorer estimates.

The experimental CN bond lengths of the group 10 mono-cyanide have similar values, around 116 pm. Recently, the CN bond lengths were experimentally determined for CrCN,⁴¹ CoCN,⁴¹ NiCN,⁴³ CuCN,¹⁸ and ZnCN.⁴⁴ Experimental values

- (30) Kraemer, W. P.; Bunker, P. R. *J. Mol. Spectrosc.* **1983**, *101*, 379.
 (31) Hirota, E. *Philos. Trans. R. Soc. London, Ser. A* **1988**, *324*, 131.
 (32) Gordy, W.; Cook, R. L. *Microwave Molecular Spectra*, 3rd ed.; Wiley: New York, 1984.
 (33) Rudolph, H. D. *Struct. Chem.* **1991**, *2*, 581.
 (34) Watson, J. K. G.; Roytburg, A.; Ulrich, W. *J. Mol. Spectrosc.* **1999**, *196*, 102.
 (35) Yamazaki, E.; Okabayashi, T.; Tanimoto, M. *J. Am. Chem. Soc.* **2004**, *126*, 1028.
 (36) Walker, N. R.; Hui, J. K.-H.; Gerry, M. C. L. *J. Phys. Chem. A* **2002**, *106*, 5803.
 (37) Yamazaki, E.; Okabayashi, T.; Tanimoto, M. *Chem. Phys. Lett.* **2004**, *396*, 150.
 (38) Evans, C. J.; Gerry, M. C. L. *J. Phys. Chem. A* **2001**, *105*, 9659.
 (39) Gutsev, G. L.; Andrews, L.; Bauschlicher, C. W., Jr. *Chem. Phys.* **2003**, *290*, 47.
 (40) Filatov, M. *Chem. Phys. Lett.* **2003**, *373*, 131.

- (41) Flory, M. A.; Field, R. W.; Ziurys, L. M. *Mol. Phys.* **2007**, *105*, 585.
 (42) Sheridan, P. M.; Flory, M. A.; Ziurys, L. M. *J. Chem. Phys.* **2004**, *121*, 8360.
 (43) Sheridan, P. M.; Ziurys, L. M. *J. Chem. Phys.* **2003**, *118*, 6370.

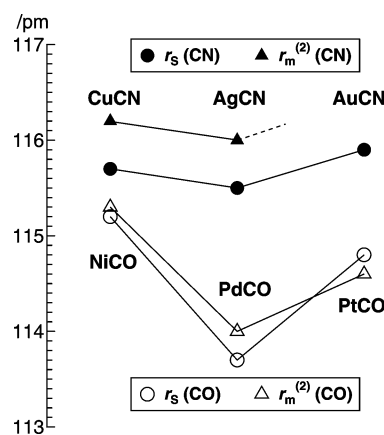
Table 4. Experimental CN Bond Lengths of Transition Metal Monocyanides (pm)

molecule	methods	with ^{15}N data	without ^{15}N data	ref
CrCN	r_0		115.29(12)	41
	r_s		114.95(35)	41
	$r_m^{(1)}$		114.8	41
CoCN ($^3\Phi_4$)	r_0		113.13(12)	42
	r_0		115.80(8)	43
NiCN	r_0		115.90(2)	43
	r_s		115.34	43
	$r_m^{(1)}$		115.2(1)	43
	$r_m^{(2)}$		114.64	44
ZnCN	r_0		114.64	44
	r_s		114.34	44
	$r_m^{(1)}$		114.17	44
CuCN	r_0	115.76(1)	115.47(14) ^a	18
	r_s	115.669(3)	115.197(11) ^a	18
	$r_m^{(1)}$	115.73(12) ^a	115.06 ^a	18
	$r_m^{(2)}$	116.213(3)		18
	r_s	115.527(67)	115.317(36)	this work
AgCN	r_s	115.4733(20)	114.944(12)	this work
	r_{IE}	115.477(28)	114.954(10)	this work
	$r_m^{(1)}$	115.525(26)	114.836(11)	this work
	$r_m^{(2)}$	116.0260(26)	115.94(51)	this work
AuCN	r_0	115.856(24)	115.89	this work
	r_s	115.86545(97)		this work

^a Calculated in the present study from rotational constants reported in ref 18.

of other transition metal monocyanides listed in Table 4 possess somewhat shorter values of around 113–115 pm. Hirano et al.^{46–49} suggested that the CN bond length of transition metal monocyanides in the ground vibrational state can be seemingly shortened because of the large amplitude effect of bending vibration (see the next subsection). The r_0 , r_s , r_{IE} , and $r_m^{(1)}$ structures are slightly more affected by zero-point vibration than the $r_m^{(2)}$ structure. Specifically, the structures of CrCN, CoCN, NiCN and ZnCN were determined from normal species together with metal-isotopomers and ^{13}C -species. The data of ^{15}N -species were not used, because it was difficult to observe ^{15}N -species in natural abundance. The mass center of a transition metal monocyanide is located near the metal atom. The coordinate of the nitrogen atom is farthest from the mass center, and the isotopic substitution of the nitrogen atom gives more accurate information on structure than the metal or carbon substitution. In fact, the CN distances, especially r_s and $r_m^{(1)}$, of CuCN and AgCN obtained without ^{15}N data are about 1 pm shorter than those obtained with ^{15}N data inclusive, as shown in Table 4. Thus, it is probable that CrCN, NiCN, and ZnCN have CN lengths similar to those of CuCN, AgCN, and AuCN, and that their dispersion is affected by the zero-point vibration. However, CoCN still seems to have too short of a CN bond, even if a systematic error is involved. It would be of much benefit to observe the spectrum of the ^{15}N -species to examine the CN bond length in more detail.

The changes in the CN bond lengths of the group 11 monocyanides and those in the CO lengths of the isoelectronic group 10 monocarbonyls are shown in Figure 5. Slightly larger

**Figure 5.** Comparison of the molecular structures in the group 11 monocyanides MCN ($M = \text{Cu},^{18}\text{Ag}, \text{and Au}$) and the isoelectronic group 10 monocarbonyls $M'\text{CO}$ ($M' = \text{Ni},^{35}\text{Pd},^{36}\text{Pt}^{38}$).**Table 5.** Nonprojected Bond Lengths and Bending Angles Obtained Using Rigid Bender Model of CuCN, AgCN, and AuCN

molecule	d_{MC} (pm) ^a	d_{CN} (pm) ^a	α (deg) ^b	ω_2 (cm ⁻¹) ^c
CuCN	183.00(23)	117.09(33)	9.5	270
AgCN	203.09(13)	116.98(19)	9.7	240
AuCN	191.08(26)	116.97(40)	8.6	320

^a Values in parentheses indicate one standard deviation. Uncertainties represent contributions from the bending vibration alone. ^b Root-mean-square displacement in α ($180^\circ - \angle\text{MCN}$) was estimated by a trial-and-error method so as to reproduce the experimental ω_2 . ^c Values reproduced from the determined constants using eqs 5 and 6. See Table 2.

variations between r_s and $r_m^{(2)}$ values were observed in the monocyanides than in the monocarbonyls. This finding could be explained by the slightly larger residual effect of the zero-point vibrations in monocyanides: the MCO species has a stiffer skeleton as a result of the double bonding character by the back-donation,^{35,37,45} illustrated as $\text{M}=\text{C}=\text{O}$. Because this back-donation is easily affected by the nature of the metal, the CO bond lengths are scattered in the group 10 monocarbonyls.³⁵ On the other hand, the CN lengths in the group 11 monocyanides are less affected because of their rigid triple bond character.

Rigid Bender Fit. Hirano et al.^{46–49} have recently suggested that experimental molecular structures reported for some transition metal monocyanides in the ground vibrational states often resulted in $r(\text{C}\equiv\text{N})$ bond lengths that were short as compared to those estimated from high-level ab initio calculations. They explained that these discrepancies were caused by the large amplitude bending-vibrational effect of the MCN molecules in the ground vibrational state. The experimental bond length reflects the projection of the bending vibration to the molecular axis. To assess their assertion, a bending potential modeling analysis was carried out using both rotational and vibrational data from higher excited bending vibrational states, $2\nu_2$, $3\nu_2$, $4\nu_2$, ... Because only the first excited state was observed in the present study, a simplified analysis using a rigid bender model would be due for the CuCN, AgCN, and AuCN molecules.

According to Walker et al.,⁵⁰ the rotational constant in the ground state, B_0 , can be expressed for a linear molecule XYZ with its molecular mass M as

(44) Brewster, M. A.; Ziurys, L. M. *J. Chem. Phys.* **2002**, *117*, 4853.

(45) Patzschke, M.; Pyykkö, P. *Chem. Commun.* **2004**, 1982.

(46) Hirano, T.; Okuda, R.; Nagashima, U.; Špirko, V.; Jensen, P. *J. Mol. Spectrosc.* **2006**, *236*, 234.

(47) Hirano, T.; Amano, M.; Mitsui, Y.; Itono, S. S.; Okuda, R.; Nagashima, U.; Jensen, P. *J. Mol. Spectrosc.* **2007**, *243*, 267.

(48) Hirano, T.; Okuda, R.; Nagashima, U.; Jensen, P. *Mol. Phys.* **2007**, *105*, 599.

(49) Hirano, T.; Okuda, R.; Nagashima, U.; Jensen, P. *J. Mol. Spectrosc.* **2008**, *250*, 33.

(50) Walker, K. A.; Evans, C. J.; Suh, S.-H. K.; Gerry, M. C. L.; Watson, J. K. G. *J. Mol. Spectrosc.* **2001**, *209*, 178.

$$B_0 = \frac{\hbar^2}{2hI_e} \left\{ 1 + \frac{m_x m_z d_{YX} d_{YZ}}{MI_e} \left[1 + \frac{m_y d_{YX} d_{YZ}}{2I_e} \right] \right\} \langle \alpha^2 \rangle \quad (4)$$

where m_x , m_y , and m_z are atomic masses, and d_{YX} and d_{YZ} are nonprojected bond lengths averaged over the ground state, which are not projections to the molecular axis, but “actual” lengths of oblique bonds. Under the assumption of the harmonic bending vibration, the bending displacement $\alpha = 180^\circ - \angle(XYZ)$ is related to the bending energy:

$$\langle \alpha^2 \rangle = L_{\alpha 2}^{-2} \langle Q_2^2 \rangle = G_{\alpha\alpha} \frac{\hbar^2}{hc\omega_2} \quad (5)$$

and

$$G_{\alpha\alpha} = \frac{MI_e}{m_x m_y m_z d_{YX}^2 d_{YZ}^2} \quad (6)$$

where $L_{\alpha 2}$ and $G_{\alpha\alpha}$ are standard Wilson matrices.⁵¹ Simultaneous fit of the B_0 values of all isotopomers yielded the bond lengths d_{YX} and d_{YZ} as listed in Table 5. However, in the present analysis, the mean-square displacement of α did not converge in the iterative process. Hence, the α values were estimated by a trial-and-error method so as to reproduce the bending vibrational energies ω_2 determined from the l -type doubling constants given in Table 2, and fixed in the subsequent least-squares analysis to obtain the bond lengths.

The nonprojected MC bond lengths averaged over the ground vibrational state were rather close to those obtained by other methods, such as r_0 and $r_m^{(2)}$ listed in Table 3. In contrast, the nonprojected CN distances, approximately 117 pm, were slightly longer than those obtained by methods such as r_0 and $r_m^{(2)}$. The nonprojected CN lengths obtained in this study were in good

agreement with those of other transition metal monocyano- nides in the ground vibrational state: FeCN (117.2 pm), CoCN (117.18 pm), and NiCN (117.05 pm), which were predicted by high-level ab initio calculations.^{47–49} Furthermore, the averaged bending displacements obtained in this study were around 9° and consistent with the values predicted for other monocyano- nides, FeCN ($10(5)^\circ$), CoCN ($8(5)^\circ$), and NiCN ($9(5)^\circ$). Our rigid bender model analysis qualitatively supports the theoretical estimates of the effective bond length affected by the zero-point vibrations for transition metal cyanides by Hirano et al.^{47–49} However, because the present analysis is not as accurate as we require, a potential modeling analysis using both rotational and vibrational data in highly excited bending vibrational states is strongly desired.

Conclusions

The physicochemical properties of monomeric AgCN and AuCN have been determined in detail through the measurement of their rotational spectra. Reliability of various theoretical calculations has been assessed for the first time through comparison between the experimental and theoretical bond distances. The present experimental results will be useful for refining metal–CN interaction models adopted in quantum chemical calculations to interpret the chemisorption of CN on a metal surface.

Acknowledgment. This study was supported by the Japan Society for the Promotion of Science through Grant-in-Aids for Scientific Research (nos. 12740316 and 15656184). E.Y.O. thanks the Hayashi Memorial Foundation for Female Natural Scientists for the Hayashi Fellowship.

Supporting Information Available: Observed transition frequencies and full citation of ref 26. This material is available free of charge via the Internet at <http://pubs.acs.org>.

JA808153G

(51) Wilson, E. B., Jr.; Decius, J. C.; Cross, P. C. *Molecular Vibrations: The Theory of Infrared and Raman Vibrational Spectra*; McGraw-Hill: New York, 1955.